Optical Materials 37 (2014) 322–326

Contents lists available at ScienceDirect

Optical Materials

journal homepage: www.elsevier.com/locate/optmat

Investigation of electronic structure and optical properties of $MgAl_2O_4$: DFT approach

A.H. Reshak [a,b], Saleem Ayaz Khan [a,*], Z.A. Alahmed [c]

[a] New Technologies – Research Centre, University of West Bohemia, Univerzitni 8, 306 14 Pilsen, Czech Republic
[b] Center of Excellence Geopolymer and Green Technology, School of Material Engineering, University Malaysia Perlis, 01007 Kangar, Perlis, Malaysia
[c] Department of Physics and Astronomy, King Saud University, Riyadh 11451, Saudi Arabia

ARTICLE INFO

Article history:
Received 29 April 2014
Received in revised form 22 May 2014
Accepted 17 June 2014
Available online 16 July 2014

Keywords:
Electronic structure
Effective mass
Chemical bonding
Optical properties

ABSTRACT

The electronic band structure, electronic charge density distribution and optical properties of $MgAl_2O_4$ were calculated using the full potential linear augmented plane wave. The exchange correlation potential was solved by recently developed modified Becke Johnson potential in the framework of DFT. The band structure and partial density of states (PDOS) were calculated. The PDOS exhibit the role of orbital in bands formation and nature of the bonds. The calculated effective mass of electrons show high mobility of electrons in the conduction band minimum with respect to heavy and light holes. The calculated electron charge density confirm the existence of mixed ionic and covalent nature of the bonds. Mg–O show more ionicity because of greater electro-negativity difference than Al–O. Imaginary part of dielectric function $\varepsilon_2(\omega)$ exhibit high transparency in the visible and infrared region. For further investigation of optical properties absorption coefficient $I(\omega)$, refractive index $n(\omega)$, reflectivity $R(\omega)$ and energy loss function $L(\omega)$ were calculated. We found reasonable agreement with the experimental data.

1. Introduction

Spinel oxides are important members of ceramics family having fascinating applications in photoelectronic, geophysics, magnetism, and irradiated environments [1,2]. Among the spinel family, magnesium dialuminium oxide ($MgAl_2O_4$) is often considered as a model of spinel structure and important for both experimentalists and theoreticians because of its various applications [2,3]. As the oxide exhibit some interesting properties like high strength and melting point, it shows less electrical loss and electrical resistively [4]. Therefore $MgAl_2O_4$ is used as electrical dielectric in refractory ceramics and irradiation resistant material. $MgAl_2O_4$ is also suitable to use as a covering material replacing the quartz glass in high pressure discharge lamps [5]. It is a promising candidate for heterogeneous catalysis [6]. The permeable form of $MgAl_2O_4$ is suitable for humidity sensor which can be used for monitoring and controlling the environment humidity and ultrafiltration membranes [7–9]. $MgAl_2O_4$ is the important component of the shallow upper mantle of the earth which plays important role in geophysics [10].

$MgAl_2O_4$ is generally taken as a model of the AB_2O_4 family materials, crystallizes in spinel structure [11]. There are several theoretical [12–21] and experimental approaches [22–31] used to study the features of $MgAl_2O_4$.

In the previous literature there is clear disagreement between experimental results and theoretical work for different parameters of the investigated compound. This gave us strong motivation to use most recent modified Becke–Johnson potential [32] with high mixing factor (0.5) in order to get close agreement with the experimental data namely; band gap, density of states and optical properties of $MgAl_2O_4$. The mBJ, a modified Becke–Johnson potential, allows the calculation of band gaps with accuracy similar to the very expensive GW calculations [32]. It is a local approximation to an atomic "exact-exchange" potential and a screening term.

2. Crystal structure and computational detail

Crystal structure of $MgAl_2O_4$ is close packed face-centered cubic (FCC) space group $Fd\bar{3}m$. Each cubic cell contains eight units [33] as shown in Fig. 1. It consist tetrahedrally coordinated Mg and octahedrally coordinated Al [34]. In the present work the lattice parameter and atomic positions are taken from experimental work of Peterson et al. [28] as shown in Table 1. We make use of full potential linear augmented plane wave (FPLAPW) method as implemented in Wien2K code [35] for calculating the electronic structure, electronic charge density and optical properties of

* Corresponding author.
E-mail address: saleemayaz_hu@yahoo.com (S.A. Khan).

http://dx.doi.org/10.1016/j.optmat.2014.06.017
0925-3467/

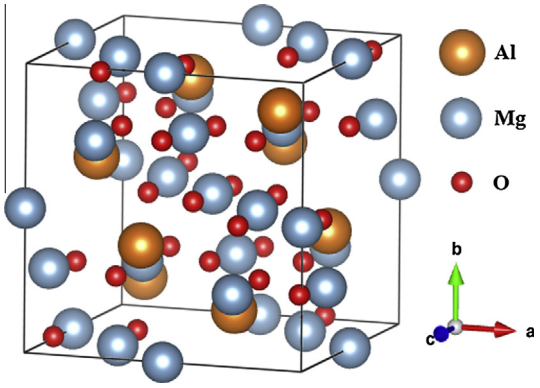

Fig. 1. Calculated unit cell of $MgAl_2O_4$.

$MgAl_2O_4$. The exchange correlation potential was treated by most recent modified Becke and Johnson (mBJ) potential [32]. In order to achieve energy eigenvalues convergence, the wavefunctions in the interstitial region were expanded in plane waves with a cutoff of $K_{max} = 7/R_{MT}$, where R_{MT} denotes the smallest atomic sphere radius and K_{max} gives the magnitude of the largest K vector in the plane-wave expansion. The R_{MT} are taken to be 1.71 atomic units (a.u.) for Mg and O atoms and 1.72 a.u. for Al atom. The valence wavefunctions inside the spheres are expanded up to $l_{max} = 10$, while the charge density was Fourier expanded up to $G_{max} = 12$ (a.u.)$^{-1}$.

We have optimized the structure by minimization of the forces (1 mRy/a.u.) acting on the atoms. From the relaxed geometry the electronic structure and the chemical bonding can be determined and various spectroscopic features can be calculated and compared with experimental data. Once the forces are minimized in this construction one can then find the self-consistent density at these positions by turning off the relaxations and driving the system to self-consistency. We have used 40 ***k***-points in the irreducible Brillouin zone for structural optimization. For calculating the total, the angular momentum decomposition of the atoms projected electronic density of states, the electron charge density distribution and the optical properties a denser mesh of 286 ***k***-points was used. The convergence of the total energy in the self-consistent calculations is taken with respect to the total charge of the system with a tolerance 0.0001 electron charges.

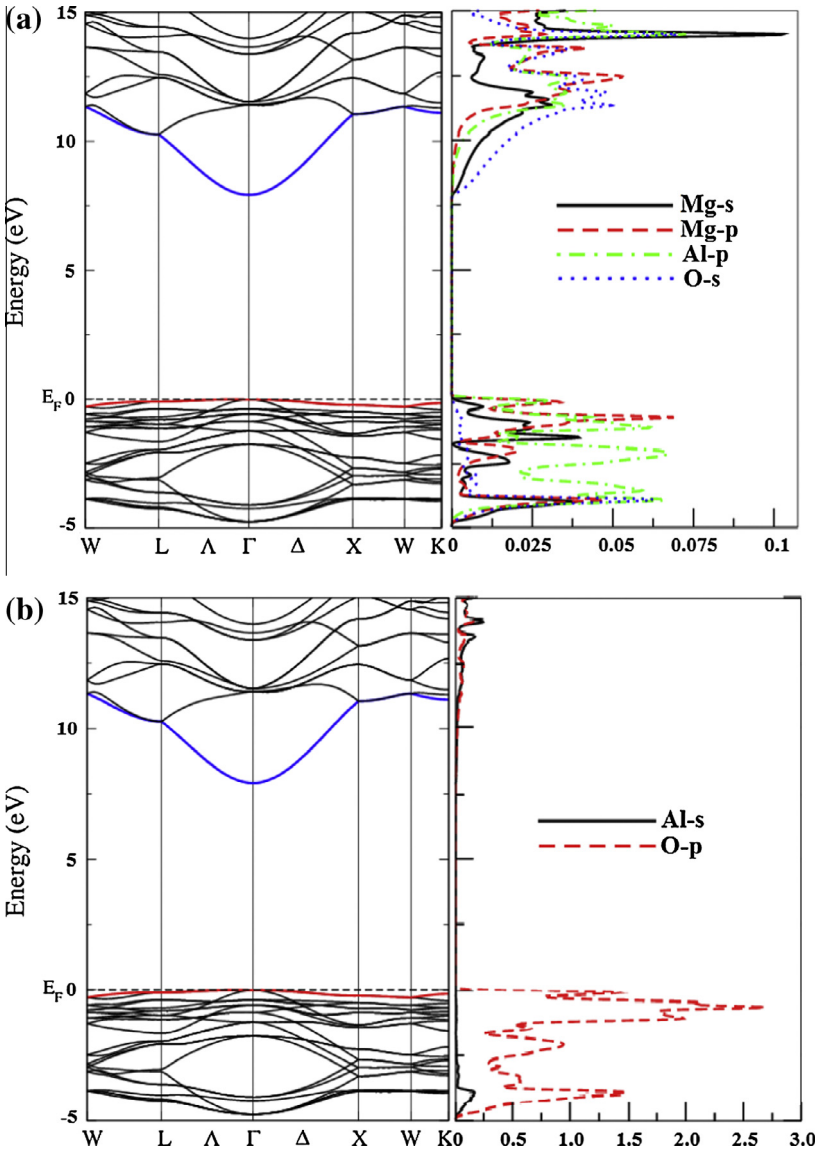

Fig. 2. Calculated band structure and partial density of states of $MgAl_2O_4$.

Table 1
Comparison of theoretical and experimental crystallographic data, band gap, and static optical constants, our calculated $n(\omega)$ is done at static limit while for the experiments were done at a wavelength vary between 350 and 650 nm.

	Atomic positions		
	Present work*	Exp [28]	Theoretical [19]
Mg	(1/8,1/8,1/8)	(1/8,1/8,1/8)	(1/8,1/8,1/8)
Al	(1/2,1/2,1/2)	(1/2,1/2,1/2)	(1/2,1/2,1/2)
O	(0.263157,0.263157,0.263157)	(0.261714,0.261714,0.261714)	(0.2632,0.2632,0.2632)
	Present work	Experimental	Theoretical
Lattice parameter (Å)	8.175*	8.085 [28]	7.905 [14], 8.027 [21],
Band gap E_g (eV)	7.8*	7.8 [28]	5.20 [18], 5.55 [19], 7.4 [20]
$n(\omega)$	1.54*	1.712–1.762 [29]	1.7320 [14]
$\varepsilon_1(0)$	2.38*	1.69–1.73 [30]	1.763 [18]
		2.89 [31]	3.00 [14], 3.112 [18]

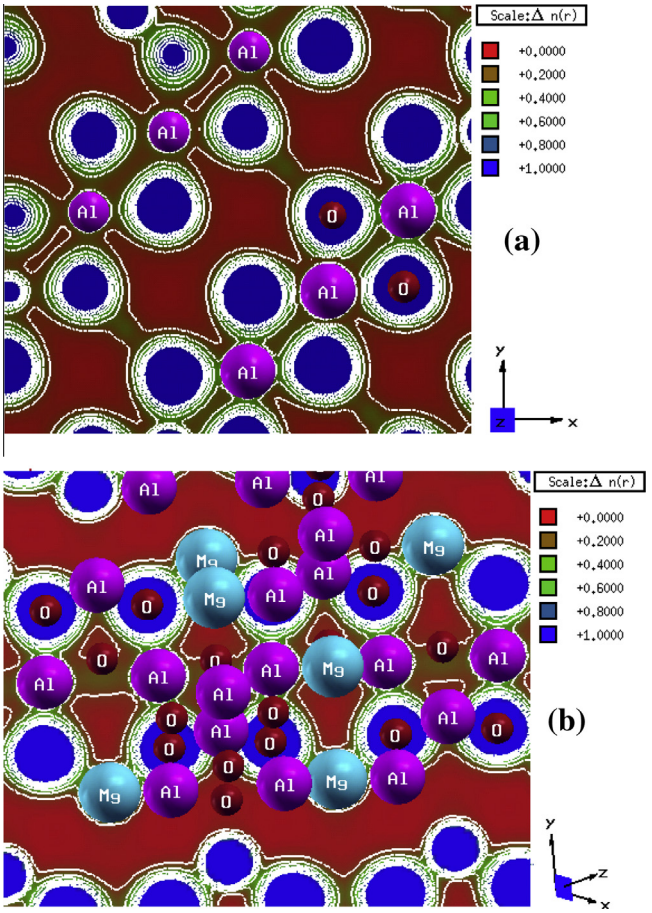

Fig. 3. Calculated valence electron charge density of $MgAl_2O_4$ (a) in (0 0 1) plane (b) in $(1\,0\,\bar{1})$ plane.

3. Result and discussion

3.1. Band structure and density of state

Band structure of the material is very important because it is correlated to the optical properties and it could help in the explanation of many physical properties of the compound. The calculated band structures along the high symmetry directions in the BZ is shown in Fig. 2a. Our calculated band gap (7.8 eV) show excellent agreement to the experimental band gap (7.8 eV) [28] as compared to the previous theoretical calculation (5.20 [18] 5.55 [19] and 7.4 eV [20]) these values are listed in Table 1. The PDOS as illustrated in Fig. 2b shows the contribution of orbitals in the bands formation. In the energy range between −5.0 eV and −4.0 eV the bands are originated from Mg-s/p, Al-s/p and O-s/p states. Mg-s/p, Al-p and O-s are strongly hybridized, the O-p state is dominant. In the energy range from −4.0 eV to −1.0 eV, the O-p state is dominant while the other states (Mg-s/p, Al-s/p and O-s) show small contribution in bands formations. From −2.50 eV to −1.12 eV the formation of the bands comes from the combination of Mg-s, Al-s/p and O-s/p states. O-p is foremost where as Al-s and O-s show negligible contribution. From −1.0 eV up to Fermi level the bands are mainly formed by hybridized Mg-p, Al-p and prevailing O-p states. The dominancy of O-p state increases the ionicity of bonds with Al and Mg. The valence band is mainly formed by O-p state (1.5 states/eV unit cell) with small contribution of Mg-p and Al-p states (0.035 states/eV unit cell). The conduction band is primarily fashioned by Mg-s and O-s states with negligible contribution of hybridized Mg-p and Al-p states. In the energy range between 12.0 eV and 14.0 eV the foremost Al-s and O-p state show strong hybridization while the weakly hybridized Mg-p, Al-p and O-s states also contribute in bands formations. From 14.0 eV to 15.0 eV, Mg-s, Al-s and O-p states are dominant while the other states show small contribution in this range. The effective mass of electron (m_e^*), heavy hole (m_{hh}^*) and light hole (m_{lh}^*) were calculated by fitting the valence and conduction bands extrema's to the parabola according to the expression $E = \frac{h^2k^2}{2m_e m^*}$ where m stands for rest mass of electron. The effective mass ratio for electrons (m_e^*/m_e), heavy holes (m_{hh}^*/m_e) and light holes (m_{lh}^*/m_e) were calculated in conduction band minimum (0.0085), upper valence band maximum (−0.2475) and lower valence band maximum (−0.3488), respectively. The calculated effective mass of electrons exhibit the high mobility of electrons in the conduction band as compared to the holes in the upper and lower valence bands.

3.2. Electronic charge density

In order to understand the bonding nature between the atoms of $MgAl_2O_4$ compound we have calculated valence electronic charge density in (0 0 1) and $(1\,0\,\bar{1})$ planes as shown in Fig. 3a and b. The bond between Al and O (Al–O) show ionic mix covalent nature. Because of greater electro-negativity difference between Al (1.61) and O (3.44) atoms, therefore the charge transfer from Al to O site, which results increases the ionicity of the Al–O bond. It is clear from the thermo-scale that the blue color show maximum charge density and red color indicate zero charge concentration. To have deep insight into the bonding nature of the investigated compound we also plotted the electronic charge density in the $(1\,0\,\bar{1})$ plane. It is clear that the (001) plane exhibit only two atoms while the $(1\,0\,\bar{1})$ plane contains all atoms of $MgAl_2O_4$. The $(1\,0\,\bar{1})$ plane have Mg–O covalent bond which is absent in (0 0 1) plane. The electro-negativity difference of Mg–O (1.73) is greater than Al–O (1.43) therefore Mg–O show more ionicity than Al–O.

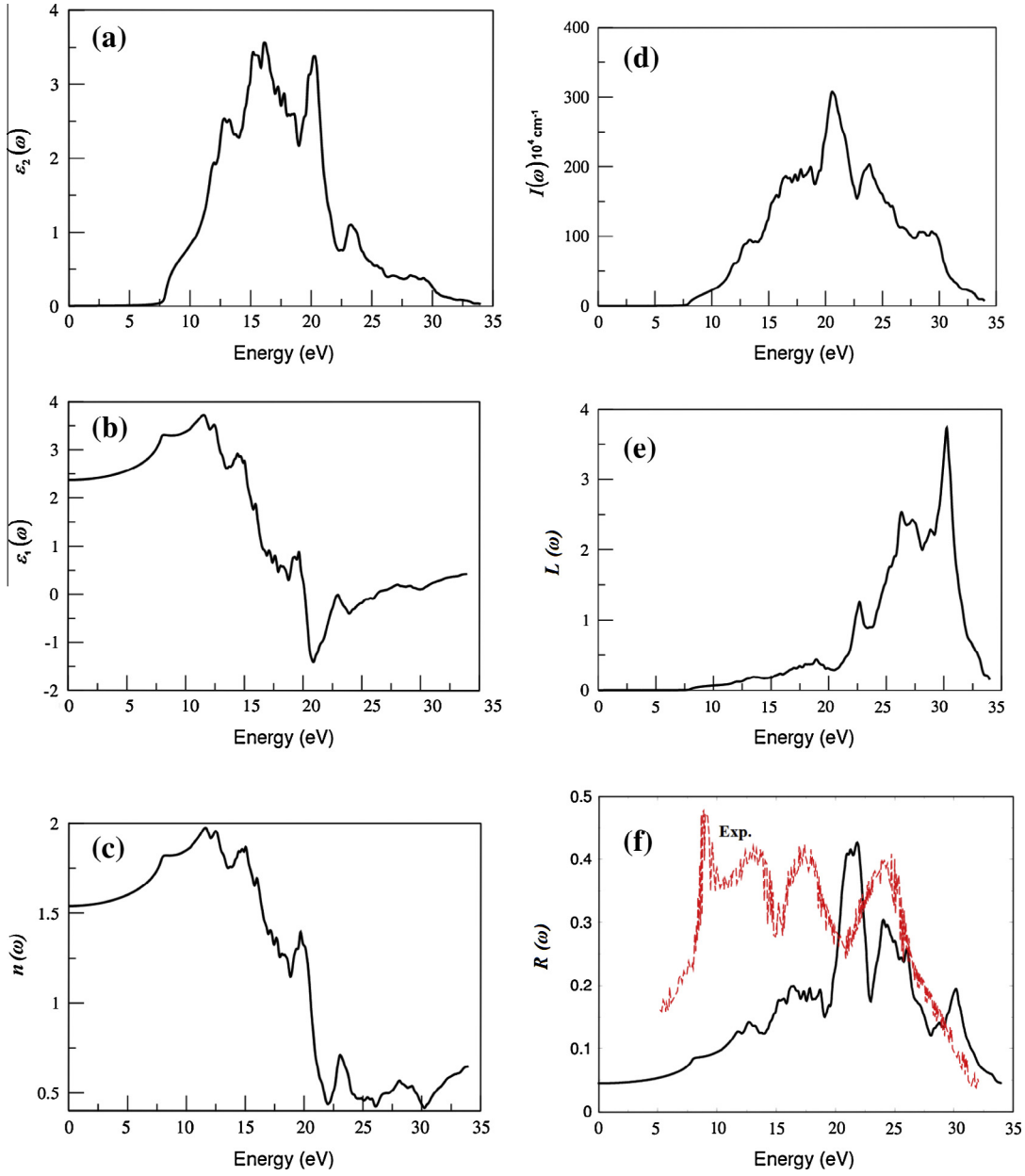

Fig. 4. (a) Calculated imaginary part of dielectric function $\varepsilon_2(\omega)$, (b) calculated real part of dielectric function $\varepsilon_1(\omega)$, (c) calculated refractive index $n(\omega)$, (d) calculated absorption coefficient $I(\omega)$, (e) calculated energy loss function $L(\omega)$ and (f) calculated reflectivity $R(\omega)$ in comparison with the experimental data [34].

3.3. Optical properties

Optical properties of solids play important role in materials research. It is impossible to get improvement in photonic devices for optical communication without proper understanding of optical properties of the materials [36,37]. The most important factor for calculating the optical properties is the complex dielectric function;

$$\varepsilon(\omega) = \varepsilon_1(\omega) + \varepsilon_2(\omega) \tag{1}$$

Dielectric function shows the electronic response of the material to electromagnetic radiations propagating in the material. The imaginary part of the dielectric function $\varepsilon_2(\omega)$ is given as [38]

$$\varepsilon_2(\omega) = \frac{4\pi^2 e^2}{m^2\omega^2 V}\sum_{v,c,k}\int_{BZ}|\langle\Psi_k^v|\vec{p}_i|\Psi_k^c\rangle|^2\delta(E_{\psi_k^c} - E_{\psi_k^v} - \hbar\omega) \tag{2}$$

where e, V and $\vec{p}_i$ represent the electronic charge, volume of unit cell and momentum operator. The quasi particle energies are represented by $E_{\psi_k^c}$ and $E_{\psi_k^v}$ and $\hbar\omega$ shows energy of the incident photons.

Fig. 4a shows the imaginary part of the dielectric function. As the compound is cubic therefore, only one component is completely identify the optical properties. In the lower energy range the material shows transparency. The absorption edge occurs at 7.8 eV which shows the first transition of electrons from valence band maximum (VBM) originated from Al-p and O-p states to conduction band minimum (CBM) formed by Mg-s, Al-s/p and O-s states. The main spectral structure is situated around 16.0 eV. The rest peaks shows transition of electron from lower to higher energy bands. The real part of dielectric function $\varepsilon_1(\omega)$ can be determined by using Kramers–Kronig relation [39]

$$\varepsilon_1(\omega) = 1 + \frac{2}{\pi}P\int_0^\infty \frac{\omega'\varepsilon_2(\omega')}{\omega'^2 - \omega^2}\,d\omega' \tag{3}$$

where P represent principal value of integral. The real part of dielectric function $\varepsilon_1(\omega)$ is shown in Fig. 4b. The spectra of $\varepsilon_1(\omega)$ shows

maximum peak at 12.0 eV. It gradually decreases with increase in photon energy and show minimum value at 22.0 eV.

Further deep into the optical properties we have calculated the refractive index $n(\omega)$, absorption coefficient $I(\omega)$, reflectivity $R(\omega)$ and energy loss function $L(\omega)$ using the relations given in [40–42].

$$n(\omega) = \left\{ \frac{\varepsilon_1(\omega)}{2} + \frac{\sqrt{\varepsilon_1^2(\omega) + \varepsilon_2^2(\omega)}}{2} \right\}^{\frac{1}{2}} \tag{4}$$

$$I(\omega) = \left\{ \sqrt{\varepsilon_1^2(\omega) + \varepsilon_2^2(\omega)} - \varepsilon_1(\omega) \right\}^{\frac{1}{2}} \tag{5}$$

$$R(\omega) = \left| \frac{\sqrt{\varepsilon(\omega)} - 1}{\sqrt{\varepsilon(\omega)} + 1} \right|^2 \tag{6}$$

$$L(\omega) = -\mathrm{Im}\left(\frac{1}{\varepsilon}\right) = \frac{\varepsilon_2(\omega)}{\varepsilon_1^2(\omega) + \varepsilon_2^2(\omega)} \tag{7}$$

The calculated refractive index $n(\omega)$ is illustrated in Fig. 4c, our calculated value of the refractive index at static limit $n(0)$ is listed in Table 1 along with the experimental [29,30] and other theoretical [14,18] results. It is clear that our calculated $n(0)$ is not well matched the experimental $n(\omega)$, that is attributed to the fact that the experimental $n(\omega)$ was obtained at a wavelength vary between 350 and 650 nm. The static part of dielectric function $\varepsilon_1(0)$ depends on band gap of the material and $\varepsilon_1(0)$ is directly linked to the $n(\omega)$ by the relation $n(\omega) = \sqrt{\varepsilon_1(0)}$. The absorption coefficient as illustrated in Fig. 4d exhibit the maximum absorption peak at 21.0 eV which corresponds to the minimum value of $\varepsilon_1(\omega)$. The energy loss spectrum is related to energy loss of fast traveling electron in the material and its value is generally large at plasma energy [43]. The dominant peak of energy loss spectrum is located at 30.0 eV. The reflectivity spectra show 4.5% reflection at 0 eV. When the photon energy is increases the reflectance of $MgAl_2O_4$ also increases and shows maximum peak with 42% reflection at 22 eV as shown in Fig. 4f. We have compared our calculated reflectivity with the experimental data [34]. We would like to mention that the difference between the magnitudes of the experimental and the theoretical curves can be made smaller if we choose a smaller broadening in our theoretical calculations. In the present calculation the broadening is around 0.1 eV.

4. Conclusions

In present work the DFT study is performed for calculating the electronic structure, electronic charge density and optical properties of $MgAl_2O_4$, using the full potential linear augmented plane wave method. The recently developed mBJ potential was used to solve exchange correlation potential. The calculated band gap show close agreement to the experimental results. The calculated PDOS provide accurate information of the bands formation and nature of the bonds. The calculated effective mass ratio of electrons, heavy holes and light holes expose the high mobility of electrons in the conduction band. The electronic charge density contours in $(0\,0\,1)$ and $(1\,0\,\bar{1})$ plane showed mixed ionic covalent bond between Al–O and Mg–O. The ionic nature of Mg–O is dominant because greater electro-negativity difference. The calculated $\varepsilon_2(\omega)$ and $I(\omega)$ shows high transparency in IR and visible region and gave response in extreme UV region. The absorption edge show the electron transitions from valence band maximum to conduction band minimum around Γ point of the BZ. The other optical constants $n(\omega)$, $R(\omega)$ and $L(\omega)$ are also calculated and discussed in detail.

Acknowledgment

The result was developed within the CENTEM project, reg. no. CZ.1.05/2.1.00/03.0088, co-funded by the ERDF as part of the Ministry of Education, Youth and Sports OP RDI program. MetaCentrum and the CERIT-SC under the program Center CERIT Scientific Cloud reg. no. CZ.1.05/3.2.00/08.0144.

References

[1] Pascal Thibaudeau, François Gervais, J. Phys. Condens. Matter 14 (2002) 3543.
[2] S.Da. Rocha, P. Thibaudeau, J. Phys.: Condens. Matter 15 (2003) 7103.
[3] U.D. Wdowik, K. Parlin' ski, A. Siegel, J. Phys. Chem. Solids 67 (2006) 1477.
[4] J.M. Leger, J. Haines, M. Schmidt, J.P. Petitet, A.S. Pereira, J.A.H. daJornada, Nature 383 (1996) 401 (London).
[5] R.J. Bratton, J. Am. Ceram. Soc. 57 (1974) 283.
[6] A. Govindaraj, E. Flahaut, C. Laurent, A. Peigney, A. Rousset, C.N.R. Rao, J. Mater. Res. 14 (1999) 2567.
[7] P.P.L. Regtien, Sens. Actuators 2 (1981/82) 85.
[8] G. Gusmano, G. Montesperelli, P. Nunziante, E. Traversa, Br. Ceram. Trans. 92 (1993) 104.
[9] A. Larbot, G. Philip, M. Persin, L. Cot, Key Eng. Mater. 132–136 (1997) 1719.
[10] T. Irifune, K. Fujino, E. Ohtani, Nature 349 (1991) 409 (London).
[11] F.S. Galasso, Structure and Properties of Inorganic Solids, Pergamon, New York, 1970.
[12] M.C. Warren, M.T. Dove, S.A.T. Redfen, Mineral. Mag. 62 (2000) 311.
[13] S.H. Wuai, S.B. Zhang, Phys. Rev. B 63 (2001) 045112.
[14] P. Thibaudeau, F. Gervais, J. Phys. Condens. Matter 14 (2002) 3543.
[15] M. Catti, G. Valerio, R. Dovise, M. Causà, Phys. Rev. B 49 (1994) 14179.
[16] R. Pandey, J.D. Gale, S.K. Sampath, J.M. Recio, J. Am. Ceram. Soc. 82 (1999) 3337.
[17] Y-N. Xu, W.Y. Ching, Ching, Phys. Rev. B 43 (1991) 4461.
[18] S.M. Hosseini, Phys. Status Solidi (b) 245 (12) (2008) 2800.
[19] M. Hachemaoui, F. Semari, R. Khenata, A. Bouhemadou, M. Rabah, Journal of Scientific Research No 0, vol. 1 (2010).
[20] B. Amin, R. Khenata, A. Bouhemadou, Iftikhar Ahmad, M. Maqbool, Physica B 407 (2012) 2588.
[21] U.D. Wdowik, K. Parlin'ski, A. Siegel, J. Phys. Chem. Solids 67 (2006) 1477.
[22] L.W. Finger, R.M. Hazen, A.M. Hofmeister, Phys. Chem. Miner. 13 (1986) 215.
[23] M.B. Kruger, J.H. Nguyen, W. Caldwell, R. Jeanloz, Phys. Rev. B 56 (1997) 1.
[24] S.K. Sampath, J.F. Cordaro, J. Am. Ceram. Soc. 81 (1998) 649.
[25] P. Fischer, Z. Kristallogr. 124 (1967) 275.
[26] V. Askarpour, M.H. Manghnani, S. Fassbender, A. Yoneda, Phys. Chem. Miner. 19 (1993) 511.
[27] Shigeto Sawai, Takashi Uchino, J. Appl. Phys. 112 (2012) 103523.
[28] R.C. Peterson, G.A. Lager, R.L. Hitterman, Am. Mineral. 76 (1991) 1455.
[29] GEMSELECT, http://www.gemselect.com/gem-info/spinel/spinel-info.php.
[30] J.H. Boo, S.B. Lee, S.J. Ku, W. Koh, C. Kim, K.S. Yu, Y. Kim, Appl. Surf. Sci. 169 (170) (2001) 581.
[31] N.N. Boguslavska, E.F. Venger, N.M. Vernidub, Yu.A. Pasechnik, K.V. Shportko, Semicond. Phys. Quantum Electron. Optoelectron. 5 (2002) 95.
[32] F. Tran, P. Blaha, Phys. Rev. Lett. 102 (2009) 226401.
[33] R.J. Hill, J.R. Graig, G.V. Gibbs, Phys. Chem. Miner. 4 (1979) 317.
[34] M.L. Bortz, R.H. French, D.J. Jones, R.V. Kasowski, F.S. Ohuchi, Phys. Scr. 41 (1990) 537.
[35] P. Balaha, K. Shewartz, G.K.H. Madsen, D. Kvsnicka, J. Luitz, WIEN2K, An Augmented Plane Wave + Local Orbitals Program for Calculating Crystals Properties, Karlheinz Schewartz, Techn. Universitat, Wien Austria, 2001, ISBN 3-9501031-1-2.
[36] J. Singh, Optical Properties of Condensed Matter and Applications, John Wiley sons, England, 2006. ISBN-13 978-0-470-02192–7 (HB).
[37] S.A. Khan, A.H. Reshak, Int. J. Electrochem. Sci. 8 (2013) 9459.
[38] M. Launay, F. Boucher, P. Moreau, Phys. Rev. B 69 (2004) 035101.
[39] H. Tributsch, Naturforsch. A 32A (1977) 972.
[40] M. Dressel, G. Gruner, Electrodynamics of Solids: Optical Properties of Electrons in Matter, Cambridge University Press, UK, 2002.
[41] A.H. Reshak, S.A. Khan, Comput. Mater. Sci. 78 (2013) 91.
[42] P. Ravindran, A. Delin, B. Johansson, O. Eriksson, J.M. Wills, Phys. Rev. B 59 (1999) 1776.
[43] P. Nozieres, Phys. Rev. Lett. 8 (1959) 1.